Chain-length dependence of lipid bilayer properties near the liquid crystal to gel phase transition

Michael R. Morrow, John P. Whitehead, and Dalian Lu
Department of Physics, Memorial University of Newfoundland, St. John's, Newfoundland, Canada A1B 3X7

ABSTRACT The temperature dependence of the mean orientational order parameter in the vicinity of the liquid crystal to gel phase transition is obtained from the first moment M_1 of deuterium nuclear magnetic resonance spectra for bilayers of chain perdeuterated phosphatidylcholines with acyl chains of 12, 14, 16, and 18 carbons. The data clearly show an increasing temperature dependence of the orientational order parameter in the vicinity of the transition, with the effect becoming more pronounced with decreasing chain length. Assuming a linear relationship between the mean orientational order parameter and the extension of the acyl chain, estimates of the change in area of the membrane at the transition are shown to be consistent with those obtained from other measurements. It is shown that the transition may be modeled in terms of a Landau expansion of the free energy involving a small number of phenomenological parameters. From this it is shown that the behavior of these systems in the temperature range of interest is, in large part, controlled by the close proximity of a spinodal to the transition temperature.

INTRODUCTION

Considerable theoretical and experimental interest has been focused on the properties of synthetic bilayer membranes comprised of phospholipid molecules, particularly the family of diacyl phosphatidylcholines. Much of the interest stems from the fact that while such systems model many of the structural features of biological membranes, they are also amenable to systematic analysis and interpretation. Of particular interest is the liquid crystalline to gel phase transition observed in these systems. Experimental evidence strongly suggests that the transition is first order (1, 2), which would imply a finite latent heat and a discontinuous change in area per lipid and in chain orientational order. Much work, both experimental (3–12) and theoretical (13–23), has dealt with the nature of fluctuations which might be manifested as an enhanced sensitivity of some parameters to temperature near the transition. The possibility of fluctuation effects has led some authors to postulate the existence of a critical point on the gel/liquid crystal coexistence curve (14, 17, 18). Some experiments suggest that the addition of certain polypeptides to the bilayer can shift the first order liquid crystal to gel transition into a continuous phase change (24, 25) which implies the existence of a critical point on the gel/liquid crystal coexistence curve of the pure lipid bilayer. The behavior of various bilayer properties as the transition is approached is often described in terms of the approach toward a spinodal point, sometimes referred to as a "pseudocritical point", lying within a few degrees of the transition temperature (6–9, 11, 22, 23, 26, 27).

One parameter which is believed to display an enhanced temperature sensitivity near the transition is area per lipid (19). Recent theoretical studies have examined the extent to which this behavior might depend on acyl chain length. An experimental parameter which can be closely related to area per lipid is the mean orientational order of the acyl chains (29–34) which, in turn, can be inferred from measurements of the first moment, M_1, of the ^{2}H NMR spectrum of chain perdeuterated lipid bilayers. There has been little systematic study of the dependence of the mean orientational order of the acyl chains on chain length in the vicinity of the transition. In the current work, we present mean orientational order parameter data from chain perdeuterated lipid bilayers for four members of the phosphatidylcholine family having acyl chains with 12, 14, 16, and 18 carbons. These are, respectively, dilauroylphosphatidylcholine (DLPC-d_{46}), dimyristoylphosphatidylcholine (DMPC-d_{54}), dipalmitoylphosphatidylcholine (DPPC-d_{62}) and distearoylphosphatidylcholine (DSPC-d_{70}). Data of this sort for DLPC-d_{46} and DSPC-d_{70} have not, to our knowledge, been previously presented. A simple comparison of mean orientational order parameter, expressed as M_1, for the four chain lengths illustrates a number of subtle points regarding chain-length dependence of the bilayer behavior. By relating M_1 to chain extension (29–34), it is possible to approximate the behavior of area per lipid near the transition. This allows the data to be interpreted in terms of a simple Landau expression for the free energy which provides an excellent description of the observed data in terms of three phenomenological parameters. While the analysis is predicated upon the assumed existence of a critical point in the liquid crystal/gel coexistence curve, we are unable to extract a meaningful estimate of the critical temperature from the data without further model dependent assumptions. The data and the subsequent analysis do however indicate that the coexistence temperature is within a few degrees of the spinodal and that this, in large part, controls the thermodynamic behavior of these systems over the temperature range of interest. We conclude the paper with a discussion of the significance of the results obtained in the present study.

MATERIALS AND METHODS

Perdeuterated fatty acids were prepared using the method of Hsiao et al. (35) and used in the synthesis of DLPC-d_{46}, DMPC-d_{54}, DPPC-d_{62}

0006-3495/92/07/18/10 $2.00

and DSPC-d_{70} using the method introduced by Gupta and co-workers (36). Samples were pumped on overnight to remove residual traces of solvent. The DPPC-d_{62} sample contained 64 mg of dry lipid. The other samples contained approximately 50 mg of dry lipid. Each sample was placed into a 0.5 ml NMR tube (8-mm diameter) and ~300 μl of 50 mM phosphate buffer (pH = 7.0) added. The suspension was warmed above the phase transition and stirred gently with a fine glass rod. Samples were checked for degradation using thin layer chromatography. All were found to run as a single spot.

^{2}H NMR spectra were obtained using a locally built spectrometer with a 3.5 T superconducting magnet supplied by Nalorac Cryogenics Corp. (Martinez, CA). Details of the spectrometer have been reported elsewhere (37). Transients were collected using the quadrupole echo sequence (38) with a pulse separation of 35 μs and a $\pi/2$ pulse length of 2 μs. For each spectrum, 2,000 transients, collected with a repetition time of 0.9 s, were averaged.

Samples were allowed to equilibrate at 76°C for ~1 h. Sample temperatures were changed in 1°C steps close to the transition and 2°C steps otherwise. After each temperature change, the sample was allowed to equilibrate for at least 30 min before collection of the transients was begun. To locate the transition more precisely, experiments were repeated on some samples with temperature steps of 0.25°C near the transition. Temperatures were controlled to ±0.05°C using a computer-based temperature controller coupled to a copper-constantan thermocouple near the sample. The accuracy of the temperatures was estimated to be better than ±0.5°C based on perdeuterated lipid transition temperatures.

In the liquid crystalline phase of a bilayer, the orientational order parameter for a given deuteron on an acyl chain is given by (39)

$$S_{CD} = {}^1/_2\langle 3\cos^2\theta_{CD} - 1\rangle, \quad (1)$$

where θ_{CD} is the angle between the carbon-deuterium bond and the rotational axis of the molecule and the average is taken over the conformations of the chain. The first moment of the half spectrum is given by

$$M_1 = \frac{\int_0^\infty d\omega\omega f(\omega)}{\int_0^\infty d\omega f(\omega)}, \quad (2)$$

where $f(\omega)$ is the spectrum. Within the liquid crystalline phase, M_1 for a chain-perdeuterated lipid is related to the mean orientational order parameter along the chain, $\overline{S_{CD}}$, by (39)

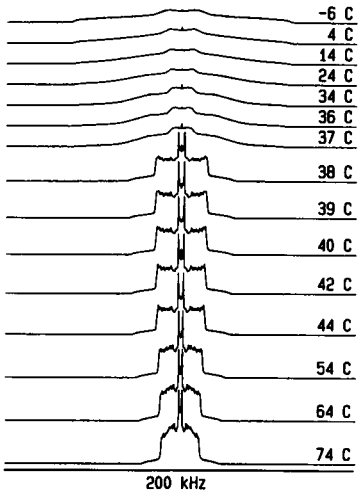

FIGURE 1 ^{2}H NMR spectra for DPPC-d_{62} at selected temperatures.

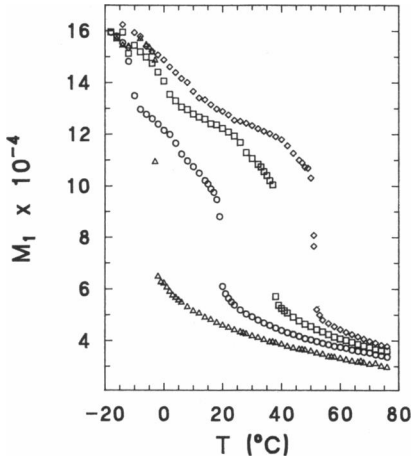

FIGURE 2 First moment M_1 versus T for (△) DLPC-d_{46}, (○) DMPC-d_{54}, (□) DPPC-d_{62}, (◇) DSPC-d_{70}.

$$M_1 = \frac{\pi}{\sqrt{3}}\frac{e^2qQ}{h}\overline{S_{CD}}, \quad (3)$$

where e^2qQ/h = 167 kHz is the quadrupole coupling for deuterium in a carbon deuterium bond. In general, there is a linear relationship between $\overline{S_{CD}}$ and acyl chain extension (29, 30). While a specific relationship of this type cannot be derived below the main transition, it is likely that for gel spectra close to the transition temperature, there is a monotonic increase in M_1 with increasing orientational order and extension of the acyl chain.

RESULTS AND DISCUSSION

Deuterium NMR measurements

^{2}H NMR spectra were recorded between 76°C and −14°C for samples of DLPC-d_{46}, DMPC-d_{54}, DPPC-d_{62} and DSPC-d_{70}. Representative spectra for DPPC-d_{62} are shown, in Fig. 1, at selected temperatures above and below the main transition. Fig. 2 shows the temperature dependence of the first spectral moment, M_1, for each of the lipids. It can be seen that at a given temperature, above the main transition, mean orientational order increases with acyl chain length. As the temperature is lowered toward the transition, mean orientational order increases. The data suggest that shorter chain lipids can accommodate more ordering than the longer chain lipids before it is energetically favorable for the bilayer to undergo a transition into the more ordered phase. The mean orientational order parameter immediately above the transition, for each lipid, is found to decrease with increasing chain length.

In Fig. 2, values of M_1 for some spectra fall between the liquid crystal and gel values at the transition. In all cases, these spectra are superpositions of the spectra corresponding to the two phases rather than spectra

characteristic of an intermediate state of the bilayer. This coexistence reflects the fact that the sample is composed of independent multilamellar vesicles which may display a small degree of heterogeneity due to size, degree of hydration, degree of deuteration, or purity. This unavoidable heterogeneity, coupled with the strong temperature dependence of M_1 in the immediate vicinity of the transition, renders precise measurement of the jump in orientational order at the transition unreliable. Nevertheless, it is apparent that, for DMPC-d_{54}, DPPC-d_{62} and DSPC-d_{70}, the magnitude of the jump in mean orientational order at the transition increases with increasing chain length. This is an important point which has received only limited attention in microscopic modeling of this transition (23, 28).

The main transitions for DMPC-d_{54}, DPPC-d_{62}, and DSPC-d_{70} seen in the data of Fig. 2 are from the liquid crystal L_α phase to the rippled phase referred to as the $P_{\beta'}$ phase. Between 5 and 10°C below the main transition, there is an additional transition from the $P_{\beta'}$ phase to the $L_{\beta'}$ phase (40). The transition between the $P_{\beta'}$ and the $L_{\beta'}$ phases is not readily apparent in plots of M_1. For the purposes of this analysis, then, the main transition is treated as occurring between the liquid crystalline phase and a gel phase with no distinction being made between $P_{\beta'}$ and $L_{\beta'}$. Each of the three longer chain lipids displays a broad transition, at lower temperature, from $L_{\beta'}$ to a more ordered phase identified as the L_c phase. The spectra in this lower phase begin to approach the axially symmetric, rigid lattice spectra characteristic of restricted rotational motion.

The behavior of DLPC is somewhat more complicated. The transition, occurring near 0°C, is known to proceed in a number of steps over a range of few degrees. The behavior has been reported to depend on sample hydration and thermal history (41–43). Below the transition region, however, the orientational order parameter is characteristic of the L_c phase. The behavior of M_1 above the transition is similar to that of the longer chain lipids and it is possible that DLPC is tending toward a liquid crystal to gel transition when the transition to the more ordered phase intervenes.

Fig. 3 shows the dependence of M_1 on reduced temperature for each of the lipids studied. It is immediately apparent that reduced temperature alone does not predict mean orientational order for different chain lengths. This observation reinforces recent comments on the utility of reduced temperature in these systems (44).

One striking feature of the data in Fig. 2 is the increase in the magnitude of the slope of M_1 versus T as the transition is approached. As the lipid chain length decreases, this increase in slope appears to proceed slightly further before the transition intervenes. A primary goal of this work was to determine the extent to which the magnitude of this effect is sensitive to acyl chain length.

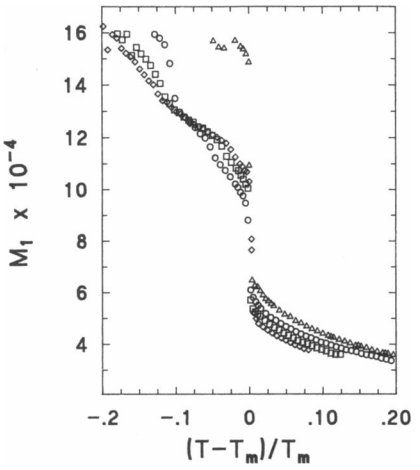

FIGURE 3 First moment M_1 versus reduced temperature $T - T_m/T_m$ for (△) DLPC-d_{46}, (○) DMPC-d_{54}, (□) DPPC-d_{62}, (◇) DSPC-d_{70}.

The first moment data also provides information regarding the dependence of the area per lipid on temperature in the liquid crystal phase near the transition. For DMPC, DPPC, and DSPC, the volume of the bilayer changes by ~0.07% per degree away from the transition and by ~4% at the transition (45). If the bilayer volume is treated as being constant, the behavior of the area per lipid may be approximated by $\langle l \rangle^{-1}$ where $\langle l \rangle$ is the extension per segment of the acyl chain along the bilayer normal. A linear relationship between orientational order parameter and extension of the acyl chain on a lattice has been derived under the assumption of axially symmetric motion by Seelig and co-workers (29, 30). Based on this relationship, we have obtained $\langle l \rangle$ from M_1 using

$$\langle l \rangle = 1.25\ \text{Å}\left[\frac{1}{2} + \frac{\sqrt{3}}{\pi 167\ \text{kHz}} M_1\right]. \quad (4)$$

Linear relationships between mean orientational order and chain extension have been used in a number of recent studies (31–33). While there has been little direct testing of this relationship, it appears to be consistent with some neutron and x-ray diffraction data on DPPC (31, 46). Recent work (34) based on measurements of area per lipid yields a numerically different relationship between $\overline{S_{CD}}$ and chain extension but the expression of that relationship in terms of area per lipid rather than chain extension complicates the comparison.

Ipsen et al. (32) have pointed out that the assumptions used to derive a relation, such as that upon which Eq. 4 is based, are not satisfied below the main transition and, indeed, give nonphysical results at very low temperatures. Nevertheless, it is reasonable to expect that some change in area per lipid occurs over a small temperature range below the main transition and that this will have some effect on the value of M_1 in the gel phase. We have

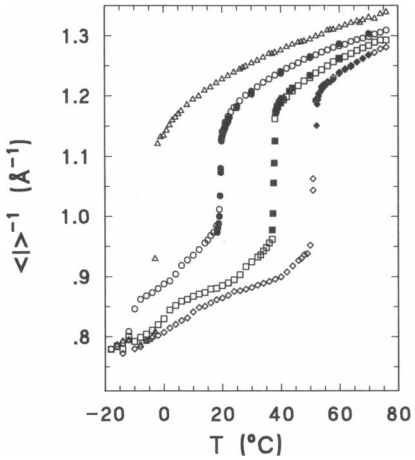

FIGURE 4 Inverse chain extension $\langle l \rangle^{-1}$ versus T. $\langle l \rangle^{-1}$ is obtained from M_1 using the relationship given in Eq. 4. (△) DLPC-d_{46}, (○) DMPC-d_{54}, (□) DPPC-d_{62}, (◇) DSPC-d_{70}. The open symbols are obtained from the data presented in Fig. 2. The solid symbols are additional data sets collected from the same samples or samples prepared in the same way from the same stock material in order to better localize the transition.

applied the transformation of Eq. 4 to all of the M_1 data including some additional runs in which the temperature was changed in smaller steps near the transition in order to better localize the transition temperature. Fig. 4 shows the temperature dependence of $\langle l \rangle^{-1}$ for the four chain lengths studied. Some care must be taken in interpreting this figure. For temperatures above the main transition, for a given lipid, $\langle l \rangle^{-1}$ can be taken as being proportional to area per lipid. At temperatures for which the sample is in the L_c phase, $\langle l \rangle^{-1}$ is certainly not proportional to area per lipid. For temperatures just below the main transition, there is no theoretical reason to expect that the values of $\langle l \rangle^{-1}$ plotted are proportional to area per lipid. Based on the arguments given by Ipsen et al. (32) one would expect the change in area per lipid to be overestimated by the relationship used to obtain Fig. 4. It is, however, very interesting to note that neutron diffraction measurements indicate that, for DPPC, the ratio of area per lipid at 20°C to area per lipid at 50°C is about 0.75 (46). X-ray diffraction measurements (40, 47) give, for the same ratio, a value of ~0.72. From Fig. 4, the ratio for DPPC of $\langle l \rangle^{-1}$ at 20°C to its value at 50°C is also ~0.72 which suggests that the extension of the relationship given by Eq. 4 into the gel phase, while not justified on theoretical grounds, may give a useful picture of how area per lipid changes immediately below the transition. In the discussion which follows, a phenomenological model is developed to represent the data shown in Fig. 4.

Modeling of the transition

A variety of theoretical models have been constructed to address phenomena associated with the liquid crystal to gel transition in lipid bilayers. Statistical mechanical models have been used to provide a microscopic picture of bilayer behavior near the transition (28, 48–52). The model presented by Marčelja (49) suggests that the first order transition occurs close to a critical point and many subsequent treatments have been more specifically concerned with the effect of fluctuations near the transition. Much of the initial effort, in this regard, was directed toward explaining the increase in ion permeability of the bilayer, near the transition, in terms of fluctuations (14, 15).

Landau models have been used extensively to provide a picture of behavior occurring near the transition including the tendency of proteins to drive the phase transition toward a critical point (18, 53–55) and the effects of interbilayer interaction (27). Landau phenomenology has also been used to address ultrasonic relaxation (5, 6) and specific heat (7, 8) near the spinodal point which, in these cases, has been referred to as a "pseudocritical" point (26). This type of analysis has also been applied to observations on ordering of water (9) and fluorescence lifetime heterogeneity (11) near the transition. Some of these studies have implied that the divergence of various quantities near the transition is "classical" (5, 6, 8, 11) and that the spinodal points lie within a few degrees of the transition temperature (6, 8).

Many theoretical studies of fluctuation effects near the transition have been based on "q-state" models where q is between 2 and 10 (14, 16, 17). Two state models have been used to account for diffusion of ions through bilayers (10, 14), the behavior of bilayers containing integral proteins (56), and the behavior of lateral compressibility and specific heat near the transition (21). Monte Carlo simulations employing a "10-state" version of this model have also been used to examine the properties of the bilayer near the transition (19, 20, 22, 23). Results from Monte Carlo calculations have also been related to the phenomenological picture in order to obtain information about the location of the spinodal (22).

In the following analysis we wish to demonstrate how a satisfactory account of the data presented in Fig. 4 and discussed in the previous section, can be provided by a simple expansion of the free energy in terms of area per lipid.

We begin our analysis by noting that the liquid crystal/gel coexistence temperature, T_m, is determined by a variety of factors that may, in principle, be varied in a continuous manner. In the subsequent analysis we wish to think not of a single coexistence temperature (namely that observed experimentally) but instead of a coexistence curve which may, in principle, be generated by continuously varying one of the factors referred to above. We furthermore assume that an increase in the coexistence temperature leads, in some sense, to a weakening of the transition which could be observed, for example, through a reduction in the latent heat asso-

ciated with the transition. Consistent with this picture is the existence of a critical point beyond which the transition from the liquid crystal state to the gel state is continuous. While the continuous variation of the coexistence temperature and the existence of a critical isotherm in such systems represents a valid theoretical generalization, direct measurement of the coexistence curve is likely impractical if not impossible. We nevertheless denote, by T_c and $\langle l \rangle_c^{-1}$, the critical temperature and the value of $\langle l \rangle^{-1}$ at the critical point respectively. Defining an order parameter s by

$$s = \frac{\langle l \rangle^{-1} - \langle l \rangle_c^{-1}}{\langle l \rangle_c^{-1}} \tag{5}$$

and noting that the magnitude of this parameter is never greater than 0.25 over the temperature region of interest, we assume that the free energy can be expanded in a power series in the order parameter s as

$$G = G_0\left[\frac{s^4}{4} + \alpha(T - T_c)\frac{s^2}{2} + \beta(T_m - T)s\right], \tag{6}$$

where $\beta > 0$ and $\alpha > 0$. The parameter G_0, which determines the overall scale of any variation in the free energy, does not enter into the present calculation and cannot be determined from any of the data presented. As shown in the Appendix, the above form of the free energy is consistent with similar expressions given in the literature (18, 25, 27, 53, 54) and represents the simplest form that nevertheless provides an adequate description of the experimental data. The expression for the free energy G given by Eq. 6 is illustrated in Fig. 5 as a function of the order parameter s for the case $T < T_c$ and $T < T_m$, $T = T_m$, or $T > T_m$. We note that for $T < T_c$ the free energy has two minima, the positions of which may be determined from the solution of the equation

$$\frac{dG}{ds} = G_0[s^3 + \alpha(T - T_c)s + \beta(T_m - T)] = 0. \tag{7}$$

For $T < T_m$ the thermodynamically stable phase yields $s < 0$ indicating that the system is the gel phase while for $T > T_m$ the thermodynamically stable state yields $s > 0$ indicating that the thermodynamically stable state is the liquid crystal state. For $T = T_m$ the two minima yield the same value for the free energy indicating that at T_m the liquid crystal and the gel phase are both thermodynamically stable from which we identify the parameter T_m as the transition temperature. At $T = T_m$, the two solutions to Eq. 7, corresponding to the minima in G, are readily obtained as

$$s_l = \sqrt{\alpha(T_c - T_m)} \tag{8}$$

$$s_g = -\sqrt{\alpha(T_c - T_m)}, \tag{9}$$

where s_l and s_g denote the values of the order parameter at the transition temperature in the liquid crystal and the gel phase respectively. Note that, in this model, the liquid crystal and gel branches of the coexistence curve are symmetric with respect to the line $s = 0$. From Eqs. 8 and 9 we obtain the result that the change in the order parameter s at the phase transition is given by

$$\Delta = s_l - s_g = 2\sqrt{\alpha(T_c - T_m)}. \tag{10}$$

Eq. 10 may be used to replace the Landau parameter α in the expression for the free energy in Eq. 6 to give

$$G = G_0\left[\frac{s^4}{4} + \frac{\Delta^2}{8}\left(\frac{T - T_c}{T_c - T_m}\right)s^2 + \beta(T_m - T)s\right], \tag{11}$$

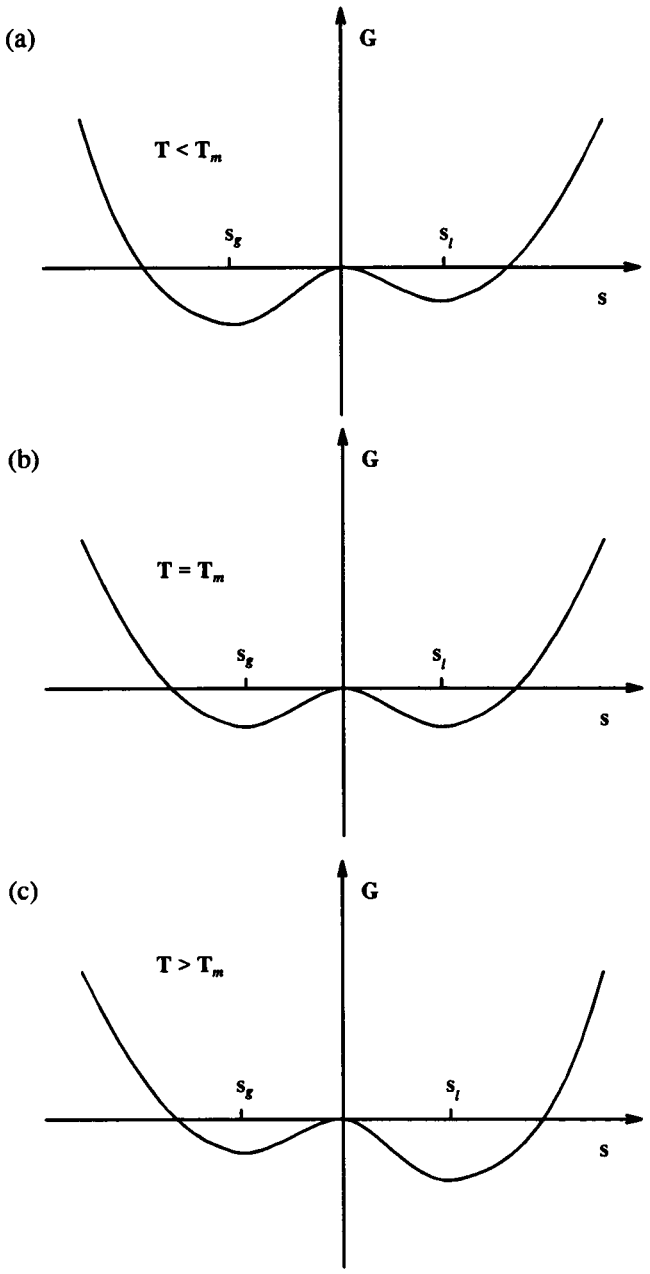

FIGURE 5 A schematic representation of the free energy versus order parameter relationship given by Eq. 6 for (*a*) $T < T_m$, (*b*) $T = T_m$, and (*c*) $T > T_m$.

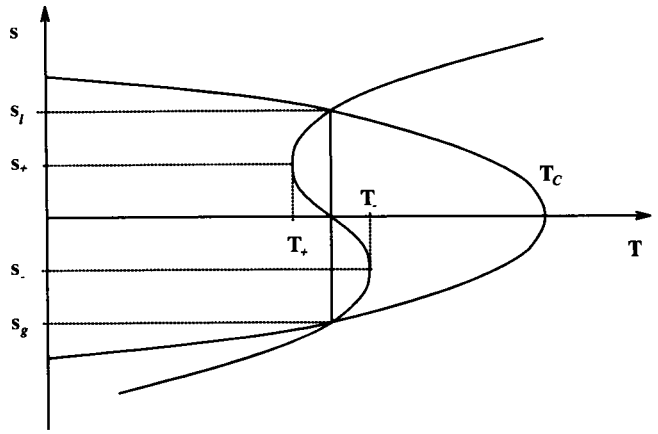

FIGURE 6 A schematic illustration of order parameter versus temperature as given by Eq. 7. The points $(T_\pm, s_\pm)$ are spinodals. The coexistence curve crosses $s = 0$ at the critical temperature T_c. The transition occurs at the coexistence temperature T_m (unlabeled) which is indicated by the solid vertical line between T_+ and T_-.

while Eq. 7, which gives the minima to the free energy, may be rewritten as

$$s^3 + \frac{\Delta^2}{4}\left(\frac{T - T_c}{T_c - T_m}\right)s + \beta(T_m - T) = 0. \tag{12}$$

The solution to Eq. 12 is plotted schematically in Fig. 6. The spinodals are shown in Fig. 6 at $s = s_\pm$ with $T = T_\pm$. The values of the order parameter s at the spinodals, $s_\pm$, are related to the spinodal temperatures, $T_\pm$, by the relation

$$\frac{d^2G}{ds^2} = G_0\left[3s_\pm^2 + \frac{\Delta^2}{4}\left(\frac{T_\pm - T_c}{T_m - T_c}\right)\right] = 0. \tag{13}$$

From this relation together with Eq. 12 we obtain the following equations

$$\left(\frac{s_\pm}{\Delta}\right)^2 = \frac{1}{12}\left(\frac{T_c - T_\pm}{T_c - T_m}\right), \tag{14}$$

and

$$s_\pm^3 = \frac{\beta}{2}(T_m - T_\pm). \tag{15}$$

The simultaneous solution of the above equations yields an explicit expression for the order parameter at the spinodal together with the corresponding spinodal temperature in terms of the Landau parameters. If however we assume that

$$|T_\pm - T_m| \ll |T_c - T_m|, \tag{16}$$

then the value of the order parameter at the spinodal is simply given by

$$s_\pm \approx \pm\frac{\Delta}{\sqrt{12}}, \tag{17}$$

while the spinodal temperatures $T_\pm$ are given by

$$T_\pm \approx T_m \mp \frac{\Delta^3}{12\sqrt{3}\beta}. \tag{18}$$

The assumption given in Eq. 16 will be used in subsequent analysis of the data in terms of the model presented.

Analysis of data

In comparing the results of the analytical model proposed in the previous section and the data displayed in Fig. 4, the comments regarding the validity, in the gel phase, of the relationship between the first moment and the average extension $\langle l \rangle$ given by Eq. 4 must be borne in mind. Our comparison of the model with the data of Fig. 4 focuses primarily on the interpretation of the liquid crystalline phase. The data in the gel phase is used, in the first instance, only to obtain an estimate of the relative change in area per lipid at the transition. As discussed above, the values obtained are consistent with other independent experimental estimates (40, 46, 47). As we will demonstrate, however, the predictions of the model show a surprising consistency with the data even in the gel phase.

Given that our primary consideration is the liquid crystal phase in the neighborhood of the phase transition and assuming that the transition temperature, T_m, is close to the spinodal temperature, T_+, as evidenced by the increasing slope of $\langle l \rangle^{-1}$ versus T as the transition is approached, we find it convenient to introduce the quantity

$$\delta = s - s_+. \tag{19}$$

By substituting $s = s_+ + \delta$ into Eq. 12, making the assumption indicated by Eq. 16, and discarding higher order terms, it is possible to obtain the relation

$$T = T_+ + \frac{(T_m - T_+)}{2}\left[3\left(\frac{\delta}{s_+}\right)^2 + \left(\frac{\delta}{s_+}\right)^3\right]. \tag{20}$$

The form of Eq. 20 suggests an approach to be taken in modeling the data. The symmetry of the model suggests that $\langle l \rangle_c^{-1}$ should be the value of $\langle l \rangle^{-1}$ at the midpoint of the transition. In practice, this parameter was chosen so that data within a few degrees of the transition, above and below, would be symmetric about the midpoint of the transition. Because the transition in DLPC is not from liquid crystal to gel, this parameter could not be estimated for that lipid and no fitting was attempted for DLPC. Using the value for $\langle l \rangle_c^{-1}$, the model order parameter, s, was determined from $\langle l \rangle^{-1}$. An initial value for s_+ was chosen using Eq. 14. Using data from the liquid crystalline phase only, plots of T versus $[3(\delta/s_+)^2 + (\delta/s_+)^3]$ were drawn. Any spectra which showed a superposition of gel and liquid crystal spectral components

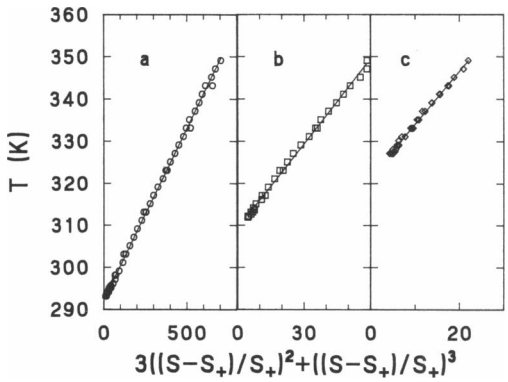

FIGURE 7 Plots of T versus $3[(s - s_+)/s_+]^2 + [(s - s_+)/s_+]^3$ in the liquid crystal phase for (*a*) DMPC-d_{54} using $\langle l\rangle_+^{-1} = 1.092$ Å^{-1}, (*b*) DPPC-d_{62} using $\langle l\rangle_+^{-1} = 1.123$ Å^{-1}, and (*c*) DSPC-d_{70} $\langle l\rangle_+^{-1} = 1.141$ Å^{-1}. The intercept gives the spinodal temperature T_+ and the slope give $(T_m - T_+)/2$. Values of $s_+ = (\langle l\rangle_+^{-1} - \langle l\rangle_c^{-1})/\langle l\rangle_c^{-1}$ were adjusted to obtain consistent values of T_+ from the slope and the intercept. Spectra which contained any gel component were omitted from this analysis.

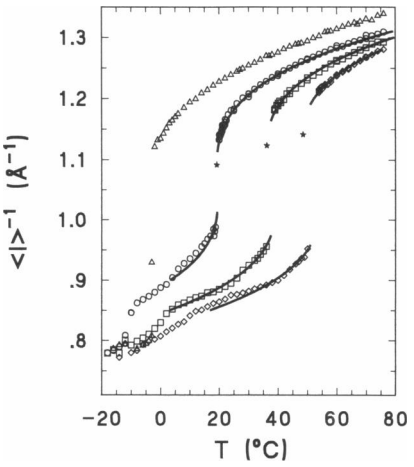

FIGURE 8 Inverse chain extension $\langle l\rangle^{-1}$ versus T. $\langle l\rangle^{-1}$ is obtained from M_1 using the relationship given in Eq. 4. (△) DLPC-d_{46}, (○) DMPC-d_{54}, (□) DPPC-d_{62}, (◇) DSPC-d_{70}. Different samples of a given lipid are not distinguished. Spectra in which gel and liquid crystal components were found to coexist have been omitted for the purposes of clarity near the transition. The solid lines are solutions to Eq. 7 obtained using parameters found with the procedure illustrated in Fig. 7 and listed in Table 1. Solid stars mark the spinodal points obtained in this way.

was omitted. The value of the order parameter at the spinodal was adjusted until the slope and intercept of the plot gave the same value for T_+ as required by Eq. 20. Such plots for DMPC, DPPC and DSPC are shown in Fig. 7. The fact that the data fall on a straight line when plotted in this way provides some assurance that this model is appropriate for these systems. The parameters associated with this fitting are displayed in Table 1. Using the values of s_+ and T_+, determined in this way, along with an estimate of Δ obtained from Eq. 14, $\langle l\rangle^{-1}$ was calculated as a function of T for DMPC, DLPC, DSPC. The resulting fits are plotted with the experimental data above and below the transition in Fig. 8. The stars indicate the positions of the spinodal point determined by the procedure outlined above. It should be emphasized that gel phase data was not used in the fitting procedure except to estimate the size of the discontinuity at the transition. The fact that the model reproduces the temperature behavior of the gel phase data over most of the range above the $L_{\beta'}$ to L_c transition is surprising. It suggests that the behavior of orientational order in these systems is particularly simple and, more surprisingly, that the relationships between mean orientational order and area per lipid retain some validity even into the gel phase. Presumably these relationships break down completely in the L_c phase where rotational motion becomes even more restricted.

TABLE 1 Fitting parameters

	DMPC	DPPC	DSPC
T_m (K)	292.5	310.65	324.15
$\langle l\rangle_c^{-1}$ (Å^{-1})	1.063	1.068	1.074
$\langle l\rangle_+^{-1}$ (Å^{-1})	1.092	1.123	1.141
T_+ (K)	292.3	309.3	321.7
$(T_m - T_+)$ (K)	0.2	1.3	2.4
$\beta \times 10^4$	2.03	2.10	2.02
$\Delta\langle l\rangle^{-1}$ (Å^{-1})	.100	.189	.232

Some observations can be made regarding the parameters listed in Table 1. It can be seen that $T_m - T_+$ decreases with decreasing chain length. While this would seem to indicate that the transition is occurring closer to the critical temperature with decreasing chain length, it is impossible to extract this information from the model. A determination of $T_c - T_m$, using Eq. 14 would require an extremely precise experimental determination of Δ. Because of the intrinsic heterogeneity of the samples and the rapid variation with temperature of M_1 near the transition, it is impossible to make this measurement with sufficient precision to separate α and $T_c - T_m$ in Eq. 10. It is intriguing, however, to note that β, which is related to the curvature of s versus T near the spinodal, is effectively independent of chain length for the group of lipids examined here. Furthermore, it is shown in the Appendix that by assuming a more restricted temperature dependence of Landau coefficients (18, 53–55), one obtains the relationship $\alpha = \beta$. If this assumption is used, the data in Table 1 yield $T_c - T_m$ values of 11°, 37°, and 58° for DMPC, DPPC and DSPC, respectively. This observation provides some justification for the assumptions implicit in Eqs. 8, 9, and 16.

The behavior of M_1, for DMPC, DPPC, and DSPC, is thus seen to be adequately reproduced between ~20 and 76°C by a classical phenomenological model for first order phase transitions. Two of the parameters, T_m and Δ, can, in principle, be measured. The chain length de-

pendence seems to be associated with these. The third parameter, β, appears to be independent of chain length.

CONCLUSIONS

First moment (M_1) data has been used to obtain the behavior of area per lipid as a function of temperature for bilayers of DLPC-d_{46}, DMPC-d_{54}, DPPC-d_{62}, and DSPC-d_{70}. The relationship between M_1 and chain extension is extended into the gel phase. While there is little theoretical justification for this extension, the result is consistent with diffraction experiments. The magnitude of the slope of area per lipid versus T is found to increase as the transition is approached. As the lipid chain length is shortened, there is a slight tendency for this change in slope to progress further before the transition intervenes.

It is possible to obtain a satisfactory description of the observed behavior by means of a simple Landau expansion of the free energy in terms of the area per lipid. Analysis of the data in terms of the model parameters indicates that the behavior of the bilayer near the transition is largely controlled by the close proximity of the spinodal temperature T_+ to the transition temperature T_m. The parameter β is found to be independent of chain length within the group of lipids examined. The value $\langle l \rangle_c^{-1}$ is found to depend only weakly on chain length. The separation between the spinodal temperature and the transition temperature decreases with decreasing chain length. This result accounts for the increasing value of the slope, at the transition, with decreasing chain length. That both the temperature difference, $T_m - T_+$ and the discontinuity in the area at the transition decrease with decreasing chain length suggests that the system is approaching a critical point as the chain length is reduced. This suggestion is further supported by the values of $T_c - T_m$ obtained by assuming a more restricted temperature dependence for the Landau coefficients as discussed above. This leads to the interesting possibility, for DLPC, that if the transition to the L_c phase did not intervene, the liquid crystal to gel transition might be of a continuous nature. While such questions cannot be addressed within the framework of the present analysis, a more detailed analysis based on a more microscopic theory may offer some insight on this matter.

It should be noted that while Eq. 4 has been used to convert M_1 to chain extension, the qualitative picture presented here is independent of the numerical details of the specific linear relationship used for the conversion.

APPENDIX

The Landau free energy used in Ref. (18) is of the form

$$G(T, u) = -a_1 u + {}^1/_2 a_2'(T - T^*)u^2 - {}^1/_3 a_3 u^3 + {}^1/_4 a_4 u^4, \quad \text{(A1)}$$

where the order parameter characterizing the transition is u and the coefficients a_1, a_2', a_3 and a_4 together with T^* are phenomenological parameters which are assumed to be independent of temperature. The equation of state, obtained by minimizing the free energy, given above, with respect to the order parameter, is

$$a_1 = a_2'(T - T^*) - a_3 u^2 + a_4 u^3. \quad \text{(A2)}$$

Equation A2 does not always provide a unique value of u for a given temperature T. In these cases, the equilibrium value of the order parameter is determined by minimizing the free energy. At the transition temperature, T_m, the equilibrium value of the order parameter changes discontinuously. This implies that there exist two solutions to the equation of state, denoted here by u_l and u_g, which yield the same value of the free energy and hence satisfy the conditions

$$G(T_m, u_g) = G(T_m, u_l), \quad \text{(A3)}$$

$$a_1 = a_2'(T_m - T^*) - a_3 u_l^2 + a_4 u_l^3, \quad \text{(A4)}$$

and

$$a_1 = a_2'(T_m - T^*) - a_3 u_g^2 + a_4 u_g^3. \quad \text{(A5)}$$

Solving Eqs. A3, A4, and A5 yields

$$T_m = T^* + \frac{2a_3^2}{9a_4 a_2'} + \frac{3a_1 a_4}{a_2' a_3}, \quad \text{(A6)}$$

$$u_l + u_g = \frac{2a_3}{3a_4} \quad \text{(A7)}$$

and

$$u_l u_g = \frac{3a_1}{a_3}. \quad \text{(A8)}$$

We note that the expression for the first order transition temperature, T_m, reduces to that given in reference 18 if we set $a_1 = 0$.

Within the model, the transition temperature and the discontinuity in the order parameter at the transition may be varied simply by changing a_1. At a critical value of this parameter,

$$a_{1c} = \frac{a_3^3}{27a_4^2}, \quad \text{(A9)}$$

the order parameters for the coexisting phases coalesce and the transition disappears and u becomes a monotonic function of T. At this critical point, the order parameters u_l and u_g both become

$$u_c = \frac{a_3}{3a_4} \quad \text{(A10)}$$

and the transition temperature is found to be

$$T_c = T^* + \frac{a_3^2}{3a_4 a_2'}. \quad \text{(A11)}$$

From the results outlined above, the equivalence between the form of the free energy given in Eq. A1 and that of Eq. 6 may readily be established by defining a reduced order parameter, s, as

$$s = \frac{u_c - u}{u_c}. \quad \text{(A12)}$$

The sign of the reduced order parameter in Eq. A12 reflects the fact that, at the transition, u changes in a direction which is opposite to that of the change in area per lipid, which is proportional to the order parameter used in this work. Identifying T_c and T_m as in Eqs. A6 and A11, the free energy given by Eq. A1 may be rewritten as

$$G = \tilde{G} + a'_2 u_c^2 (T_m - T)s + {}^1/_2 a'_2 u_c^2 (T - T_c)s^2 + {}^1/_4 a_4 u_c^4 s^4. \quad \text{(A13)}$$

This is equivalent to free energy given in Eq. 6 if we identify

$$\alpha = \beta = a'_2 u_c^2. \quad \text{(A14)}$$

It should be noted that the equality of the coefficients α and β implicit in the above derivation follows from the assumption that the Landau coefficients, particularly a_1, are independent of temperature. Relaxing this assumption leads to the more general form of the free energy given by Eq. 6 in which the coefficients α and β are not necessarily equal.

This work was supported by the Natural Sciences and Engineering Research Council of Canada and the Medical Research Council of Canada. The authors wish to thank Professors Myer Bloom, James H. Davis, and Naeem Jan for helpful discussions. Many of the deuterated lipid samples used in this study were kindly donated by Professor Davis. Some components incorporated into the NMR spectrometer were donated by Xerox Research Centre of Canada.

Received for publication 1 August 1991 and in final form 25 February 1992.

REFERENCES

1. Davis, J. H. 1979. Deuterium magnetic resonance study of the gel and liquid crystalline phases of dipalmitoyl phosphatidylcholine. *Biophys. J.* 27:339–358.
2. MacKay, A. L. 1981. A proton NMR moment study of the gel and liquid-crystalline phases of dipalmitoyl phosphatidylcholine. *Biophys. J.* 35:301–313.
3. Freire, E., and R. Biltonen. 1978. Estimation of molecular averages and equilibrium fluctuations in lipid bilayer systems from the excess heat capacity function. *Biochim. Biophys. Acta.* 514:54–68.
4. Mitaku, S., A. Ikegami, and A. Sakanishi. 1978. Ultrasonic studies of lipid bilayer. Phase transitions in synthetic phosphatidylcholine liposomes. *Biophys. Chem.* 8:295–304.
5. Mitaku, S., and T. Date. 1982. Anomalies of nanosecond ultrasonic relaxation in the lipid bilayer transition. *Biochim. Biophys. Acta.* 688:411–421.
6. Mitaku, S., T. Jippo, and R. Kataoka. 1983. Thermodynamic properties of the lipid bilayer transition. Pseudocritical phenomena. *Biophys. J.* 42:137–144.
7. Hatta, I., K. Suzuki, and S. Imaizumi. 1983. Pseudo-critical heat capacity of single lipid bilayers. *J. Phys. Soc. Jpn.* 52:2790–2797.
8. Hatta, I., S. Imaizumi, and Y. Akutsu. 1984. Evidence for weak first-order nature of lipid bilayer phase transition from the analysis of pseudo-critical specific heat. *J. Phys. Soc. Jpn.* 53:882–888.
9. Hawton, M., and J. W. Doane. 1987. Pretransitional phenomena in phospholipid/water multilayers. *Biophys. J.* 52:401–404.
10. Georgallas, A., J. D. MacArthur, X.-P. Ma, C. V. Nguyen, G. R. Palmer, M. A. Singer, and M. Y. Tse. 1987. The diffusion of small ions through phospholipid bilayers. *J. Chem. Phys.* 86:7218–7226.
11. Ruggiero, A., and B. Hudson. 1989. Critical density fluctuations in lipid bilayers detected by fluorescence lifetime heterogeneity. *Biophys. J.* 55:1111–1124.
12. Biltonen, R. L. 1990. A statistical-thermodynamic view of cooperative structural changes in phospholipid bilayer membranes: their potential role in biological function. *J. Chem. Thermodynamics.* 22:1–19.
13. Nagle, J. F. 1976. Theory of lipid monolayer and bilayer phase transitions: effect of headgroup interactions. *J. Membr. Biol.* 27:233–250.
14. Doniach, S. 1978. Thermodynamic fluctuations in phospholipid bilayers. *J. Chem. Phys.* 68:4912–4916.
15. Nagle, J. F., and H. L. Scott. 1978. Lateral compressibility of lipid mono- and bilayers. Theory of membrane permeability. *Biochim. Biophys. Acta.* 513:236–243.
16. Caillé, A., D. Pink, F. de Verteuil, and M. J. Zuckermann. 1980. Theoretical models for quasi-two-dimensional mesomorphic monolayers and membrane bilayers. *Can. J. Phys.* 58:581–611.
17. Pink, D., A. Georgallas, and M. J. Zuckermann. 1980. Phase transitions and critical indices of a phospholipid bilayer model. *Z. Physik B Condensed Matter.* 40:103–110.
18. Jähnig, F. 1981. Critical effects from lipid-protein interactions in membranes. I. Theoretical description. *Biophys. J.* 36:329–345.
19. Mouritsen, O. G., A. Boothroyd, R. Harris, N. Jan, T. Lookman, L. MacDonald, D. A. Pink, and M. J. Zuckermann. 1983. Computer simulation of the main gel-fluid phase transition of lipid bilayers. *J. Chem. Phys.* 79:2027–2041.
20. Mouritsen, O. G. 1983. Studies on the lack of cooperativity in the melting of lipid bilayers. *Biochim. Biophys. Acta.* 731:217–221.
21. Stein-Barana, A. M., G. G. Cabrera, and M. J. Zuckermann. 1984. Study of a model for the main phase transition of lipid bilayers using the Kikuchi cluster method. *Can. J. Phys.* 62:935–942.
22. Mouritsen, O. G., and M. J. Zuckermann. 1985. Softening of lipid bilayers. *Eur. Biophys. J.* 12:75–86.
23. Ipsen, J. H., K. Jørgensen, and O. G. Mouritsen. 1990. Density fluctuations in saturated phospholipid bilayers increase as the acyl-chain length decreases. *Biophys. J.* 58:1099–1107.
24. Morrow, M. R., and J. H. Davis. 1988. Differential scanning calorimetry and ^{2}H NMR studies of the phase behavior of gramicidin-phosphatidylcholine mixtures. *Biochemistry.* 27:2024–2032.
25. Morrow, M. R., and J. P. Whitehead. 1988. A phenomenological model for lipid-protein bilayers with critical mixing. *Biochim. Biophys. Acta.* 941:271–277.
26. Ikeda, H. 1979. Pseudo-critical dynamics in first-order transition. *Prog. Theor. Physics.* 61:1023–1033.
27. Goldstein, R. E., and S. Leibler. 1989. Structural phase transitions of interacting membranes. *Phys. Rev. A.* 40:1025–1035.
28. Kambara, T., and N. Sasaki. 1984. A self-consistent chain model for the phase transitions in lipid bilayer membranes. *Biophys. J.* 46:371–382.
29. Seelig, A., and J. Seelig. 1974. The dynamic structure of fatty acyl chains in a phospholipid bilayer measured by deuterium magnetic resonance. *Biochemistry.* 13:4839–4845.
30. Schindler, H., and J. Seelig. 1975. Deuterium order parameters in relation to thermodynamic properties of a phospholipid bilayer. A statistical mechanical interpretation. *Biochemistry.* 14:2283–2287.
31. Bloom, M., and O. G. Mouritsen. 1988. The evolution of membranes. *Can. J. Chem.* 66:706–712.
32. Ipsen, J. H., O. G. Mouritsen, and M. Bloom. 1990. Relationships between lipid membrane area, hydrophobic thickness, and acyl chain orientational order. The effects of cholesterol. *Biophys. J.* 57:405–412.
33. Thurmond, R. L., S. W. Dodd, and M. F. Brown. 1991. Molecular areas of phospholipids as determined by ^{2}H NMR spectroscopy. Comparison of phosphatidylethanolamines and phosphatidylcholines. *Biophys. J.* 59:108–113.
34. Boden, N., S. A. Jones, and F. Sixl. 1991. On the use of deuterium nuclear magnetic resonance as a probe of chain packing in lipid bilayers. *Biochemistry.* 30:2146–2155.

35. Hsiao, C. Y. Y., C. A. Ottaway, and D. B. Wetlaufer. 1980. Preparation of fully deuterated fatty acids by simple method. *Lipids.* 9:813–815.

36. Gupta, C. M., R. Radhakrishnan, and H. G. Khorana. 1977. Glycerophospholipid synthesis: improved general method and new analogs containing photoactivable groups. *Proc. Natl. Acad. Sci. USA.* 74:4315–4319.

37. Morrow, M. R. 1990. Transverse nuclear spin relaxation in phosphatidylcholine bilayers containing gramicidin. *Biochim. Biophys. Acta.* 1023:197–205.

38. Davis, J. H., K. R. Jeffrey, M. Bloom, M. Valic, and T. P. Higgs. 1976. Quadrupolar echo deuteron magnetic resonance spectroscopy in ordered hydrocarbon chains. *Chem. Phys. Lett.* 42:390–394.

39. Davis, J. H. 1983. The description of membrane lipid conformation, order and dynamics by ^{2}H-NMR. *Biochim. Biophys. Acta.* 737:117–171.

40. Janiak, M. J., D. M. Small, and G. G. Shipley. 1979. Temperature and compositional dependence of the structure of hydrated dimyristoyl lecithin. *J. Biol. Chem.* 254:6068–6078.

41. Finegold, L., and M. A. Singer. 1986. The metastability of saturated phosphatidylcholines depend on acyl chain length. *Biochim. Biophys. Acta.* 855:417–420.

42. Morrow, M. R., and J. H. Davis. 1987. Calorimetric and nuclear magnetic resonance study of the phase behavior of dilauroylphosphatidylcholine/water. *Biochim. Biophys. Acta.* 904:61–70.

43. Finegold, L., W. A. Shaw, and M. A. Singer. 1990. Unusual phase properties of dilauryl phosphatidylcholine (C12PC). *Chem. Phys. Lipid.* 53:177–184.

44. Lafleur, M., P. R. Cullis, and M. Bloom. 1990. Modulation of the orientational order profile of the lipid acyl chain in the L_α phase. *Eur. Biophys. J.* 19:55–62.

45. Nagle, J. F., and D. A. Wilkinson. 1978. Lecithin bilayers. Density measurements and molecular interactions. *Biophys. J.* 23:159–175.

46. Zaccai, G., G. Buldt, A. Seelig, and J. Seelig. 1979. Neutron diffraction studies on phosphatidylcholine model membranes. II. Chain conformation and segmental disorder. *J. Mol. Biol.* 134:693–706.

47. Lis, L. J., M. McAlister, N. Fuller, R. P. Rand, and V. A. Parsegian. 1982. Interactions between neutral phospholipid bilayer membranes. *Biophys. J.* 37:657–666.

48. Nagle, J. F. 1973. Theory of biomembrane phase transitions. *J. Chem. Phys.* 58:252–264.

49. Marčelja, S. 1974. Chain ordering in liquid crystals. II. Structure of bilayer membranes. *Biochim. Biophys. Acta.* 367:165–176.

50. Jacobs, R. E., B. S. Hudson, and H. C. Andersen. 1977. A theory of phase transitions and phase diagrams for one- and two-component phospholipid bilayers. *Biochemistry.* 16:4349–4359.

51. Scott, H. L. 1981. Phosphatidylcholine bilayers. A theoretical model which describes the main and the lower transitions. *Biochim. Biophys. Acta.* 643:161–167.

52. Leermakers, F. A. M., and J. M. H. M. Sheutjens. 1988. Statistical thermodynamics of association colloids. I. Lipid bilayer membranes. *J. Chem. Phys.* 89:3264–3274.

53a. Leermakers, F. A. M., and J. M. H. M. Sheutjens. 1988. Statistical thermodynamics of association colloids. III. The gel to liquid phase transition of lipid bilayer membranes. *J. Chem. Phys.* 89:6912–6924.

53. Owicki, J. C., M. W. Springgate, and H. M. McConnell. 1978. Theoretical study of protein-lipid interactions in bilayer membranes. *Proc. Natl. Acad. Sci. USA.* 75:1616–1619.

54. Owicki, J. C., and H. M. McConnell. 1979. Theory of protein-lipid and protein–protein interactions in bilayer membranes. *Proc. Natl. Acad. Sci. USA.* 76:4750–4754.

55. Priest, R. G. 1980. Landau phenomenological theory of one and two component phospholipid bilayers. *Mol. Cryst. Liq. Cryst.* 60:167–184.

56. Pink, D. A. 1984. Theoretical studies of phospholipid bilayers and monolayers. Perturbing probes, monolayer phase transitions, and computer simulations of lipid-protein bilayers. *Can. J. Biochem. Cell Biol.* 62:760–777.